

Bending Fracture Behavior of AZ31 Magnesium Alloy Fabricated by Multi-Directional Forging

Akihiro Takahashi

Department of Mechanical Engineering

National Institute of Technology (KOSEN), Miyakonojo College, Miyakonojo, Miyazaki 885-8567, Japan

Masakazu Kobayashi

Department of Mechanical Engineering

Toyohashi University of Technology, Toyohashi, Aichi 441-8580, Japan

Hiromi Miura

Department of Mechanical Engineering

Toyohashi University of Technology, Toyohashi, Aichi 441-8580, Japan

Abstract—Multi-directional forging (MDFing) method was applied to a hot-extruded AZ31 magnesium (Mg) alloy up to a maximum cumulative strain of $\Sigma\Delta\varepsilon = 2.4$. The MDFing temperature was decreased pass by pass from 623 K to 493 K. In this way, various specimens MDFed to cumulative strains of 0, 0.8, 1.6 and 2.4 were fabricated. The average grain size decreased as cumulative strain increased due to continuous dynamic recrystallization. It was confirmed that MDFing was effective to the uniform evolution of fine and equi-axed microstructure of AZ31Mg alloy. Three-point bending and other tests were conducted to each MDFed specimen to investigate mechanical properties and fundamental bending fracture behavior. The bending strength, such as $\sigma_{b,y}$ and $\sigma_{b,z}$ increased as the grain refinement progressed. The relationship between bending property, $\sigma_{b,y}$, and grain size, D , could be approximated by Hall-Petch relationship: $\sigma_{b,y} = \sigma_0 + kD^{-1/2}$, where σ_0 was 85 MPa and k was 0.21 MPa/m^{-1/2}. These material constants were in accordance with the previous report on proof stress obtained from uniaxial tensile test. Fracture behavior under multiaxial stress state was discussed based on the results of SEM observation nearby crack initiation regions and absorbing energy evaluated from bending load-displacement curves.

Keywords –magnesium alloy, multi-directional forging, microstructure, three point bending test, fracture behavior

I. INTRODUCTION

Replacement of conventional structural materials to light-weight ones are important for weight reduction of products to improve fuel efficiency and emission in transportation and logistics systems. Carbon dioxide gas (CO₂) emissions of new passenger cars registered in Europe are monitored in order to meet the objectives of an EU regulation [1]. A program outlined in the political guidelines on effluent control is demonstrated by The European Green Deal [2]. It aims to make Europe the first climate-neutral continent by 2050. According to the program, transport accounts for a quarter of the EU's greenhouse gas emissions, and still growing. To achieve climate neutrality, a 90 % saving in transport emissions is needed by 2050 such as rail, aviation, waterborne and transport fields [2]. Therefore, there is a growing trend to substitute conventional steel and ferrous cast iron for nonferrous materials especially in transport and passenger car parts. Magnesium (Mg) alloys hold promise for light-weight structural applications in transportations due to their low density as well as higher specific modulus and strength, and simultaneously can be benefited to weight reduction of transportation mechanics. However, Mg alloys are classified as hard plastic deformation materials because of a limited ductility and formability at room temperature due to the hexagonal crystal structure [3].

Recently, microstructural control, especially grain refinement by thermo-mechanical treatment under warm atmosphere, is one of the effective techniques for improving mechanical property. There have been various researches aiming at improving the ductility and strength of Mg alloys through grain refinement using various treatments of severe plastic deformation (SPD) processes e.g., Multi-Directional Forging (MDFing) [4], Equal Channel Angular Press (ECAP) [5] and High Pressure Torsion (HPT) [6]. Xing et al [7] have reported that the ultrafine grained (UFGed) AZ31 Mg alloy produced by MDFing under warm temperatures, where its grain size is approximately 0.3 μm at cumulative strain of $\Sigma\Delta\varepsilon = 5.6$, reaches tensile ductility (20 %) and strength (530 MPa) at

room temperature. Miura et al [8] represented that UFGed AZ61 Mg alloy MDFed up to $\Sigma\Delta\varepsilon = 4.0$ exhibited a superior balance of tensile ductility of over 20 % and tensile strength of 440 MPa. Recently, Miura et al [9] have applied MDFing to AZ80 Mg alloy to a cumulative strain of $\Sigma\Delta\varepsilon = 1.5$ and could achieve tensile ductility of about 22 % and tensile strength of 445 MPa at a tensile strain rate of $3.0 \times 10^{-2} \text{ s}^{-1}$ at room temperature. As above mentioned, MDFing for Mg alloys is almost carried out at warm temperatures because of the intrinsic embrittlement property of Mg alloys at room temperature. MDFing at warm temperature is essentially enabled by occurrence of dynamic recrystallization (DRX) to cause grain refinement as well as increasing number of slip systems. The grain refinement allows further MDFing at lower temperatures with the aid of grain-boundary sliding to induce development of much finer-sized microstructures. Although uniaxial tensile/compressive tests of MDFed Mg alloys [3-9] have been well reported including authors [10], researches on the bending test under multiaxial plastic stress are few. The purpose of present study is to investigate fracture behavior at the front tip regions of V-notch of the room-temperature bending specimen of AZ31 Mg alloys fabricated by MDFing. And the relationship between fracture behavior and evolved microstructure is precisely discussed.

II. EXPERIMENTAL PROCEDURE

A commercial hot-extruded AZ31 Mg bar (i.e. nominal composition of Mg-3Al-1Zn) alloy was used as the starting material. The rectangular-shaped samples with initial dimensions of $a = 14 \text{ mm}$, $b = 31 \text{ mm}$ and $c = 21 \text{ mm}$ (i.e. axial ratio of $a : b : c = 1.00 : 2.22 : 1.49$) were machine-cut so that first forging axis became parallel to the extrusion direction (see Fig.1). The sample was warm-deformed by MDFing technique at an initial strain rate of $3 \times 10^{-3} \text{ s}^{-1}$ with changing forging axis by 90° from pass to pass under decreasing temperature conditions from 623 to 493 K (see Fig.2). A pass strain of $\Delta\varepsilon = 0.8$ was applied at each forging pass. MDFing has a merit that the axis ratio of the original sample is geometrically unchanged at each pass. The samples were MDFed to various cumulative strains up to $\Sigma\Delta\varepsilon = 2.4$ at maximum. In this way, four kinds of samples MDFed to cumulative strains of $\Sigma\Delta\varepsilon = 0, 0.8, 1.6, 2.4$ were prepared. Lubricant of molybdenum disulfide paste was applied on the forging die surface to prevent any forging defects such as bulging and galling of the samples. MDFing could be carried out without any damage or evolution of heterogeneous deformation microstructure on surfaces, where the latter should indicate homogeneous deformation of samples. Fig.3 shows the die structure for MDFing in present study. As shown in Fig.4, three-point bending testing

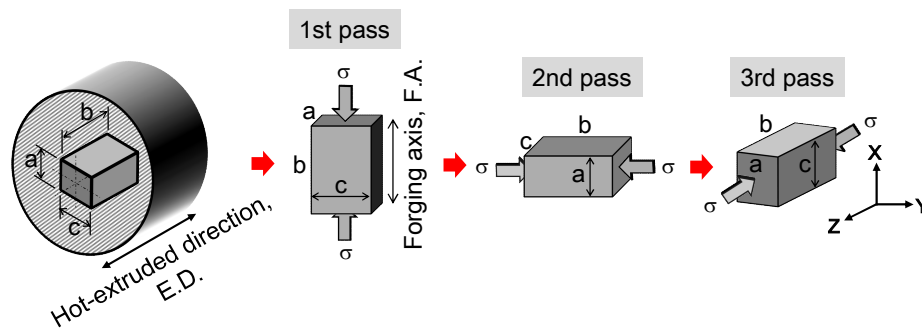


Figure 1. Schematic illustration of MDFing up to 3rd pass forging. Forging axis is varied by 90° from pass to pass (i.e. X to Y to Z). A pass strain of $\Delta\varepsilon = 0.8$ is applied at each forging.

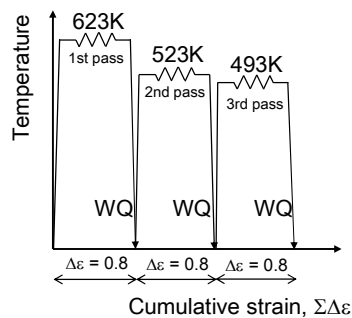


Figure 2. MDF profile in present study

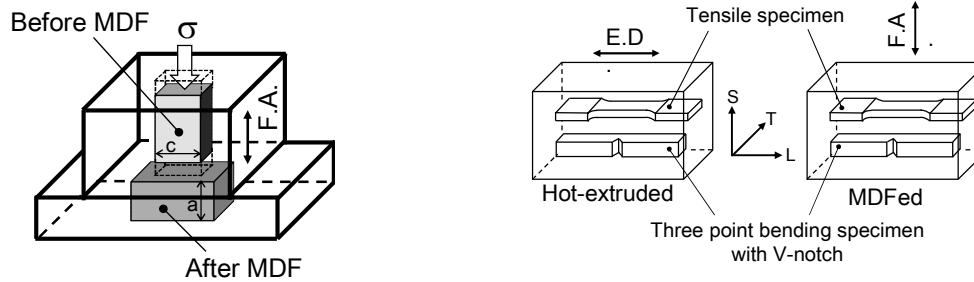


Figure3.Schematic illustration of adie for MDFing Figure 4. Sampling orientation at each specimen

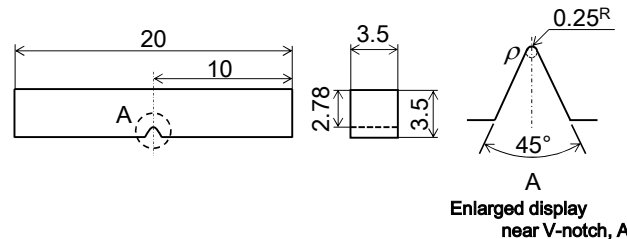


Figure5.Showing illustration of the configuration and dimensions of the three point bending specimen with V-notch in present study

specimen with V-notch normal to the extrusion direction (E.D.) was machine-cut from the hot-extruded sample. The longitudinal direction of the bending specimens MDFed was also made to correspond to direction perpendicular to the final forging axis (F.A.) (see Fig.4). Quasi-static three-point bending test was carried out at initial loading speed of 1.0 mm/min at room temperature. Fig.5 shows the configuration and dimensions of the bending specimen. Three bending specimens were prepared at each sample. Quasi-static uniaxial tensile test was carried out at initial strain rate of $2.8 \times 10^{-3} \text{ s}^{-1}$ at room temperature. Gage dimensions of tensile testing specimen were breadth of 3 mm, length of 6 mm and thickness of 2 mm. Foil strain gage was adopted to determine the 0.2 pct. proof stress. Micro-Vickers hardness test was conducted under conditions with indentation load of 7.35 N and keeping time for 15 s.

The microstructural evolution after MDFing was confirmed through optical microscope (OM) observation. The samples for metallography were mechanically polished and then etched in a solution containing acetic acid of 10 ml, picric acid of 12.5 g, distilled water of 20 ml and ethanol (95%) of 200 ml. Average grain size was measured by the linear line-intercept method [11,12] from OM and scanning electron microscope (SEM) images. SEM was used to observe entire fracture surface and deformed regions at around the front tip of V-notch after bending test.

III. RESULTS AND DISCUSSIONS

3.1. Tensile properties and evolved microstructural –

Tensile properties such as elastic modulus, 0.2 pct. proof stress, tensile strength, strain to failure and micro-Vickers hardness are given in Table 1. Drastic changes in the 0.2 pct. proof stress and the strain to failure after 1st pass of forging were confirmed comparing with those of the as-extruded sample. Fig.6 shows the evolved microstructures in the samples. Average grain size, D , decreases by straining and with decreasing temperature; initial grain size of 16.7 μm of the as-extruded sample decreases to 9.2 μm after 1st pass forging at 623 K, 5.8 μm after 2nd pass forging at 523 K and 3.5 μm after 3rd pass forging at 493 K. The homogeneous grain refinement and the decrease in grain size with decreasing MDFing temperature is a result of dynamic recrystallization, where achieved grain size is controlled by diffusion and grain-boundary migration [13]. Fig.7 shows enlarged views in the frames of A and B in Figs.6 (a) and (b), respectively. Grain boundaries (GBs) in the microstructure evolved in the as-extruded sample were somewhat smooth outline. However, the GBs after the 1st pass forging pass were corrugated and, still more, fine grains were developed on or at around the corrugated boundaries. Yang et al [14] have reported that initial coarse grains in Mg alloy are fragmented by kink bands evolved at early stages of deformation up to $\epsilon = 0.12$. Their research summarized that new fine grains in Mg alloy were formed due to a series of strain-induced continuous reaction (i.e., continuous dynamic recrystallization, cDRX). The applied strain of $\epsilon = 0.8$ by one pass

forging in the present study exceeded the above critical value reported by Yang et al. In any case, MDFing process is effective to make finer and homogeneous microstructure with low density dislocation of AZ31Mg alloys. In such fine-grained microstructures with an average grain size smaller than 1 μm , grain-boundary sliding affects plastic deformability to cause large ductility in addition to strengthening at room temperature [4, 9]. Nevertheless, the $\sigma_{0.2}$ after the first pass of forging drastically lowered than that of the as-extruded sample. This was the result of loss of texture strengthening [9]. That is, sharp basal texture developed in the as-extruded sample affected much for strengthening along extrusion direction, and it was weakened by cDRX, kinking and twinning to cause orientation randomization. However, $\sigma_{0.2}$ and ϵ_u were gradually raised with increasing cumulative strain and decreasing grain size (see Table 1). This tendency becomes more notable with further decreasing grain size [4, 9].

Table 1. The results of the tensile mechanical properties and hardness

Sample	Cumulative strain, $\Sigma\Delta\epsilon$	Elastic modulus, E, GPa	0.2 pct Proof stress, $\sigma_{0.2}$, MPa	Tensile strength, σ_u , MPa	Fracture strain, ϵ_u , (Pct)	Micro-Vickers Hardness, HV
Hot-extruded	0	45	206	258	25.8	53
1st pass	0.8	42	117	254	34.4	55
2nd pass	1.6	43	159	268	31.4	59
3rd pass	2.4	45	194	285	28.9	61

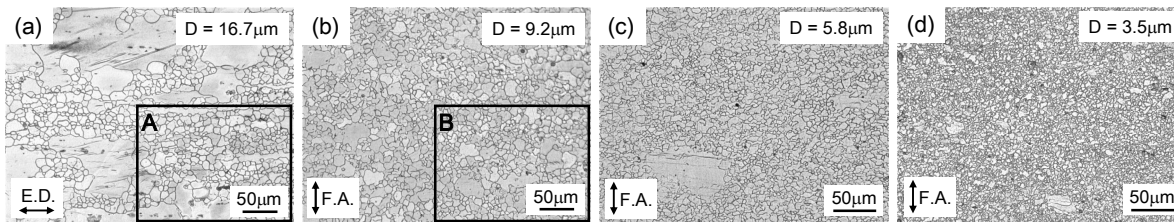


Figure 6. Microstructural change with increasing cumulative strain by MDFing: (a) as hot-extruded ($\Sigma\Delta\epsilon = 0$), (b) 1st pass ($\Sigma\Delta\epsilon = 0.8$), (c) 2nd pass ($\Sigma\Delta\epsilon = 1.6$), and (d) 3rd pass ($\Sigma\Delta\epsilon = 2.4$). Arrows indicate (a) extruded direction and (b), (c), (d) the final forging axes of MDFing, respectively.

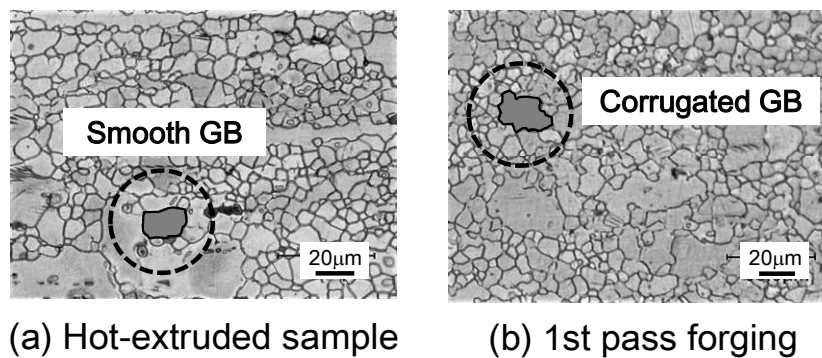


Figure 7. The enlarged views of the frame A and B in the Fig. 6 (a) and (b), respectively

3.2 Three point bending property–

Fig. 8 shows typical load-displacement curves of the three-point bending test examined at room temperature. The all curves indicated elastic-plasticity response. The bending properties such as yield load, P_y , and maximum load, P_{max} , evidently increased as the grain size decreased. In the present study, bending stress, σ_b is expressed as follows:

$$\sigma_b = \frac{3PS}{2bh^2} \quad (1)$$

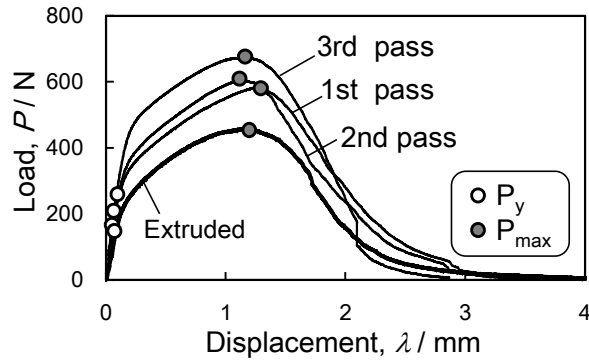


Figure8. Typical load-displacement curves obtained by three-point bending tests. Sample names are labeled to each curve.

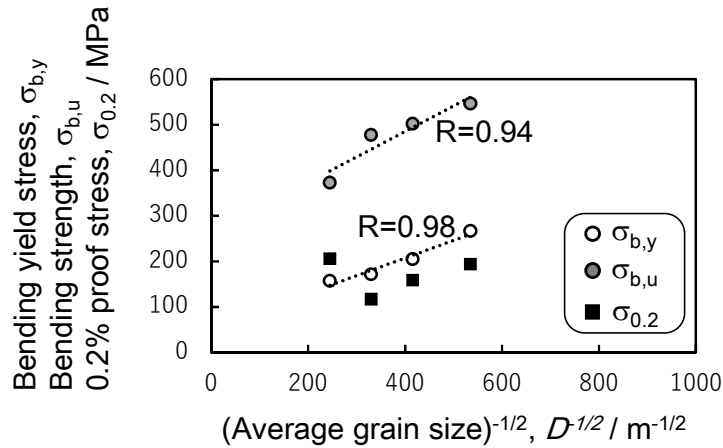


Figure9. Relationship between three kinds of mechanical properties, $\sigma_{b,y}$, $\sigma_{b,u}$, $\sigma_{0.2}$ and grain size, D , in each sample.

where P is applied load during the bending test, S is span length of 14.6 mm, b and h are the breath and height of the bending specimen. Fig.9 shows the bending yield stress, $\sigma_{b,y}$, the bending strength, $\sigma_{b,u}$, and 0.2 pct. proof stress, $\sigma_{0.2}$, for tensile test depending on grain size. It was seen obviously that the $\sigma_{b,y}$ and $\sigma_{b,u}$ increased as the grain size decreased with a high correlation coefficient, R . The tensile 0.2 pct. proof stress, in contrast, did not show clear grain-size dependency. Stress triaxiality [15-17], T , in eq. (2) is well known as an index for evaluating the height of multiaxiality under a multiaxial stress generated by restraint from the examination surroundings.

$$T = \frac{\sigma_m}{\bar{\sigma}} \quad (2)$$

where σ_m is hydrostatic stress and $\bar{\sigma}$ is equivalency stress of Von Mises. σ_m and $\bar{\sigma}$ are given by following eq. (3) and (4):

$$\sigma_m = \frac{1}{3}(\sigma_1 + \sigma_2 + \sigma_3) \quad (3),$$

$$\bar{\sigma} = \sqrt{\frac{(\sigma_1 - \sigma_2)^2 + (\sigma_2 - \sigma_3)^2 + (\sigma_3 - \sigma_1)^2}{2}} \quad (4),$$

where σ_1, σ_2 and σ_3 are the maximum principal stress, intermediate principal stress and minimum principal stress, respectively. Therefore, the stress triaxiality, $T = 1/3$ becomes under uniaxial stress (i.e., tensile test using smooth gauge specimen). T is larger than $1/3$ as the multiaxiality increases under the multiaxial stress in which the tension stress field acts in all directions of the surroundings. Uniaxial tensile tests at quasi-static strain rate were carried out by one of the authors under conditions of stress triaxiality of $T = 0.33$ to 1.39 using circumferential notched specimens of hot-extruded AZ61 Mg alloy [18]. As a result, it was found that the yield stress, σ_y , was increased with increasing the stress triaxiality, T , with correlation coefficient $R = 0.98$. Thus, it was concluded that yield stress of Mg alloy at early stage of plastic deformation greatly related to stress triaxial state rather than microstructural texture. Closer experiment on this point should conduct in the future.

The relationship among the bending properties, $\sigma_{b,y}$, $\sigma_{b,u}$ and the grain size, D , can be approximated by following Hall-Petch relationship:

$$\sigma_{b,y} = \sigma_0 + kD^{-1/2} \quad (5),$$

$$\sigma_{b,u} = \sigma_0 + kD^{-1/2} \quad (6).$$

For $\sigma_{b,y}$, σ_0 and k are evaluated to be 85 MPa and $0.21 \text{ MPa/m}^{-1/2}$. And for $\sigma_{b,u}$, σ_0 and k are 262 MPa and $0.56 \text{ MPa/m}^{-1/2}$, respectively. Yuan et al. [19] and Koike et al. [20] have reported that the relationships between yield stress, σ_y , and grain size, D , for several Mg alloys could be given by following Hall-Petch coefficients; $\sigma_0 = 103 \text{ MPa}$ and $k = 0.24 \text{ MPa/m}^{-1/2}$ [19], and $\sigma_0 = 90\text{-}210 \text{ MPa}$ and $k = 0.17 \text{ MPa/m}^{-1/2}$ [20]. The data of σ_0 and k in the present study approximately similar to the above coefficients.

On the other hand, according to Timoshenko and Gere [21], the relationship between the plastic moment, M_p , and the yield moment, M_y , of an elastic-perfectly plastic material (non-hardened elasto-plastic material) is expressed by the following eq.:

$$f = \frac{M_p}{M_y} \quad (7),$$

where f is commonly called the shape factor. Yield moment, M_y , for a rectangular beam is,

$$M_y = \sigma_y \frac{bh^2}{6} \quad (8),$$

in the inelastic bending theory of a beam based on an elastic-perfectly plastic material, it assume that σ_y is equal to the 0.2 pct. proof stress in uniaxial tensile test and the factor, $f = 1.5$. Thus, the ratio of $\sigma_{b,u}/\sigma_{0.2} = 1.5$ can be evaluated from the series of this theory. It is interesting that the ratio is the range of 1.3 to 1.5 within the grain sizes attained by MDFing in the present study.

3.3 Fracture surface observation–

Fractography by SEM was carried out and typical photographs are displayed in Fig.10. Figs.10 (a) and (d) exhibit dissociation characteristics with metallurgical slip orientation for deformation in the as-extruded specimen. There are a large number of the river patterns in very different directions, the cleavage terraces and a few small dimples on the surfaces. It was suggested that a lot of large slip bands and profuse twinning were developed along to certain orientations in the grain interior in the as-extruded specimen. SEM photographs in Figs.10 (b) and (c) show mostly ductile fracture surface with dense dimples in both MDFed specimens, where dimples of resembling comet shape look aligned upward (see Figs.10 (e) and (f)). Dimple fracture basically occurs to decrease stress concentration in intensely developed plastic regions. Furthermore, the multiaxial stress state in the internal necking within the plastic region urges shear stress component. Arrows in white color near the V-notch root indicate secondary microcrack extended in vertical to the photographs. These microcracks lead to an increase in extrinsic deformation. Therefore, it was suggested that the equivalency stress of Von-Mises stress, $\bar{\sigma}$ (i.e., shear strain energy) in the front of V-notch increases due to occurrence of the microcracks. In addition, the loss of texture strengthening took place by MDFing [9], leading to reduction of flow stress. This is corresponding to decrease of 0.2 pct. proof stress at 1st pass forging less than that at hot-extruded.

Area of ductile shear zone of the extruded specimen is smaller than that of the 3rd pass MDFed specimen. Larger shear zone ahead of the V-notch tip can be explained increasing of absorbing energy during three point bending fracture process. Absorbing energy, E_f , can be determined from load-displacement curve in Fig.8 by

evaluating these integral. As results, the E_t increases as MDFing pass steps up: the values of E_t of the specimens of as-extruded, 1st pass forging, 2nd pass forging and 3rd pass forging are 0.77 J, 1.01 J, 1.00 J and 1.11 J, respectively.

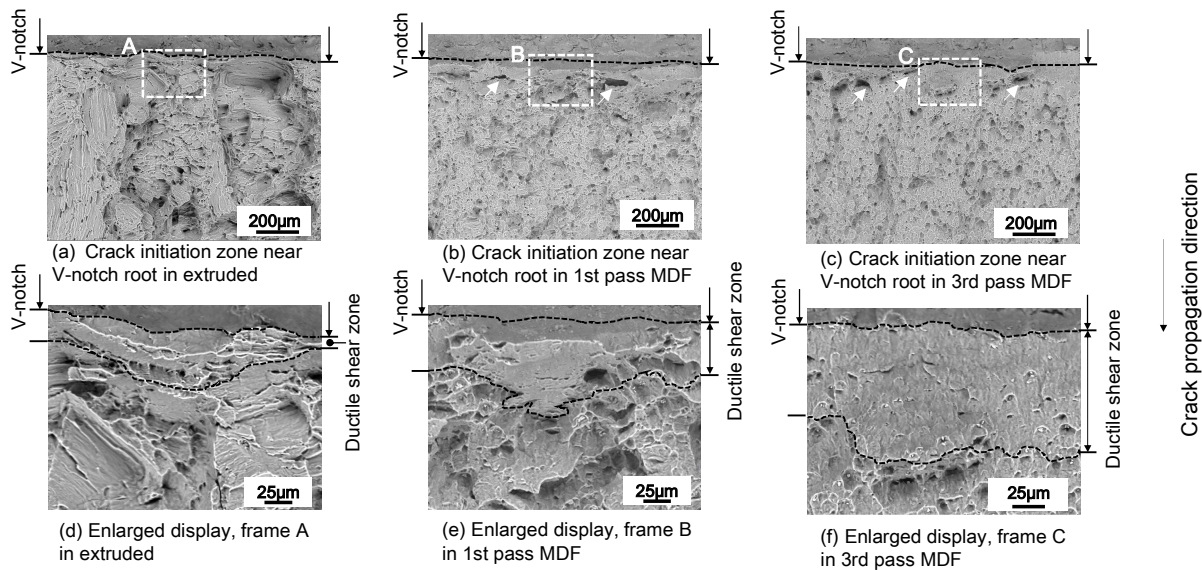


Figure 10. SEM micrographs of the fracture surfaces near V-notch root; specimens of (a) and (d) hot-extruded, (b) and (e) 1st pass MDF, (c) and (f) 3rd pass MDF. (d), (e) and (f) are the enlarged images of the frames A, B and C in (a), (b) and (c). Main crack propagation direction is indicated by white arrows. Areas surrounded by black-dashed lines in (d), (e) and (f) show brittle fracture manner.

IV. CONCLUSION

Multi-Multi-directional forging (MDFing) process under decreasing temperature conditions from 623 to 493 K was adopted to attain finer-grain sized microstructure and improve bending strength of AZ31 Mg alloy. Three-point bending test using specimens with V-notch and other mechanical tests as well as metallographic microstructural observation were carried out by using hot-extruded sample and various MDFed ones up to cumulative strain of $\Sigma\Delta\varepsilon = 2.4$ at maximum. After bending tests, fracture behavior was investigated relating with mechanical properties and grain size. The results are summarized as follows:

1. The average grain size decreased as cumulative strain increased due to occurrence of continuous dynamic recrystallization. It was confirmed that MDFing technique was effective to the evolution of finer and homogeneous microstructure of AZ31Mg alloy.
2. The bending strength, such as $\sigma_{b,y}$ and $\sigma_{b,u}$ increased as grain size decreased. The relationship between the bending property, $\sigma_{b,y}$, and the grain size, D , could be approximated by Hall-Petch relationship: $\sigma_{b,y} = \sigma_0 + kD^{-1/2}$, where σ_0 was 85 MPa and k was 0.21 MPa/m^{-1/2}. Both σ_0 and k were well corresponding to the results of proof stress obtained from uniaxial tensile tests.
3. Fracture surface of bending specimen in the as-extruded specimen showed intensely dissociation characteristics with metallurgical slip orientation. The fracture surface in the MDFed specimen exhibited mostly shear dimple fracture. Ductile shear zone near crack initiation region in the MDFed specimen was larger than that in the as-extruded one. Therefore, it was found that the equivalency stress of Von-Mises stress, $\bar{\sigma}$ (i.e., shear strain energy), in the front of V-notch increases due to appearance of the equi-axed fine grain to cause orientation randomization and reduce anisotropy of plastic deformation. Because of this effect, absorbing energy increased as MDFing pass stepped up.

Acknowledgments

This study was supported by Toyohashi University of Technology (Research No. 2107 and 2103) and the AMADA foundation (AF-2019025-B3). The authors also appreciate the financial assistance of the Light Metal Educational Foundation, Japan.

REFERENCES

- [1] G. Mellios, S. Hausberger, M. Keller, C. Samarasinghe and L. Ntziachristos, "Parameterisation of Fuel Consumption and CO₂ Emissions of Passenger Cars and Light Commercial Vehicle for Modelling Purposes", *JRC Scientific and Technical Reports*, 2-6, 2011
- [2] The European Green Deal, "COMMUNICATION FROM THE COMMISSION TO THE EUROPEAN PARLIAMENT, THE EUROPEAN COUNCIL, THE COUNCIL, THE EUROPEAN ECONOMIC AND SOCIAL COMMITTEE AND THE COMMITTEE OF THE REGIONS", *European Commission, COM(2019) 640 final*, 10-11, 2019
- [3] S. Yi, "Mechanical Anisotropy and Deep Drawing Behaviour of AZ31 and ZE10 Magnesium Alloy Sheets", *Acta Mater.*, vol. 58, 592-605, 2010
- [4] J. Xing, X. Yang, H. Miura and T. Sakai, "Mechanical Properties of Magnesium Alloy AZ31 after Severe Plastic Deformation", *Mater. Trans. J.*, vol. 49, 69-75, 2008
- [5] H. Watanabe, A. Takara, H. Somekawa, T. Mukai and K. Higashi, "Effect of Texture on Tensile Properties at Elevated Temperatures in an AZ31 Magnesium Alloy", *Scr. Mater.*, vol. 52, 449-454, 2005
- [6] M. Kai, Z. Horita, T. G. Langdon, "Development Grain Refinement and Superplasticity in a Magnesium Alloy Processed by High-Pressure Torsion", *Mater. Sci. Eng. A.*, vol. 488, 117-124, 2008
- [7] J. Xing, X. Yang, H. Miura and T. Sakai, "Ultra-Fine Grain Development in an AZ31 Magnesium Alloy during Multi-Directional Forging under Decreasing Temperature Conditions", *Mater. Trans. JIM.*, vol. 46, 1646-1650, 2005
- [8] H. Miura, G. Yu, X. Yang and T. Sakai, "Microstructure and Mechanical Properties of AZ61 Mg Alloy Prepared by Multi Directional Forging", *Trans. Nonferrous Metals Sci. China*, vol. 20, 1294-1298, 2010
- [9] H. Miura, M. Kobayashi and T. Benjanarasuth, "Effects of Strain Rate during Multi-Directional Forging on Grain Refinement and Mechanical Properties of AZ80Mg Alloy", *Mater. Trans.*, vol. 57, 1418-1423, 2016
- [10] A. Takahashi, H. Miura and M. Kobayashi, "Tensile Fracture Behavior in Wrought Magnesium Alloy Fabricated by Multi-Directional Forging Technique", *International Journal of Innovations in Engineering and Technology*, vol. 13, Issue. 3, 117-123, 2019
- [11] H. Abrams, "Practical Applications of Quantitative Metallography", *ASTM STP 504*, 138-182, 1972
- [12] George F. Vander Voort, "Metallography Principles and Practice", *New York, ASM International*, 435-471, 1999
- [13] T. Sakai, A. Belyakov, R. Kaibyshev, H. Miura, J.J. Jonas, "Dynamic and post-dynamic recrystallization under hot, cold and severe plastic deformation conditions", *Progress in Materials Science*, vol. 60, 130-207, 2014
- [14] X. Yang, H. Miura and T. Sakai, "Dynamic Evolution of New Grains in Magnesium Alloy AZ31 during Hot Deformation", *Mater. Trans.*, vol. 44, No. 1, 197-203, 2003
- [15] P.W. Bridgman, "Studies in Large Plastic Flow and Fracture", *First Edition, McGraw-Hill Company Inc.*, 1952
- [16] E.A. Davis and F. M. Connelly, "Stress Distribution and Plastic Deformation in Rotating Cylinders of Strain-Hardening Material", *Journal of Applied Mechanics*, vol. 26, No. 1, 25-30, 1959
- [17] Y. C. Deng, G. Chin, X. F. Yang and T. Xu, "Strain Limit Dependence on Stress Triaxiality for Pressure Vessel Steel", *7th International Conference on Modern Practice in Stress and Vibration Analysis, Journal of Physics, Conference Series*, 181-012071, 2009
- [18] R. Kawano, K. Hiroike, A. Takahashi, N. Yamamoto and T. Toyohiro, "Notch Effects on Tensile Properties in an AZ31 Magnesium Alloy", *6th International Conference on Science, Technology and Education 2020*, 16-20, 2020
- [19] W. Yuan, S. K. Panigrahi, J. Q. Su and R. S. Mishra, "Influence of Grain Size and Texture on Hall-Petch Relationship for a Magnesium Alloy", *Scr. Mater.*, vol. 65, 994-997, 2011
- [20] J. Koike, "Strength and Ductility of Mg Alloys", *Proc. of the 4th Pac. Rim Int. Conf. of Advanced Mater. and Processing*, 1179-1182, 2001
- [21] S. P. Timoshenko and J. M. Gere, "Mechanics of Materials", *D. Van Nostrand Company*, 289-316, 1972